Hindawi Publishing Corporation
Journal of Sensors
Volume 2012, Article ID 640780, 5 pages
doi:10.1155/2012/640780

Research Article

Theoretical Study on the Detection of Tilted Lipid Bilayers Using Surface Plasmon Resonance Techniques

Koyo Watanabe and Koji Matsuura

Research Core for Interdisciplinary Sciences, Okayama University, 3-1-1 Tsushima-Naka, Kita-Ku, Okayama 700-8530, Japan

Correspondence should be addressed to Koyo Watanabe, kouyouwatanabe@gmail.com

Received 12 October 2011; Revised 18 January 2012; Accepted 18 January 2012

Academic Editor: Chao-Min Cheng

Effective refractive indices detected using surface plasmon resonance techniques are calculated as a function of the tilt angle of lipid bilayers in a multilayered model. The changes in the effective refractive indices are derived from the shift of an excitation angle of surface plasmon. To obtain effective refractive index plots, we determined refractive index changes in the lipid bilayers with 3 and 5 nm thicknesses as a function of tilt angle and obtained a relationship between the effective refractive index and tilt angle. We also showed that the effective refractive index depended on the lipid bilayers thickness and anisotropic permittivities, which vary with interchain distance.

1. Introduction

Mechanical stimuli (MS) such as osmotic stress, membrane stretch, and shear force are activators for cellular functions including signaling, proliferation, impulse propagation, and gene expression [1]. MS are believed to induce formation changes in the cell membrane, leading to conformational changes in membrane proteins [2, 3]. For instance, in the cardiovascular system, transient receptor potential membrane proteins, which act as mechanosensitive ion channels, are activated by blood pressure [4]. Furthermore, in the field of mammalian reproduction, it has been confirmed that reproductive cells can be activated by shear stress caused by embryo and/or fluid motions [5]. Although unique relationships between MS and cellular activation have been reported, no study has yet provided a clear understanding of the mechanism at the molecular level.

In lipid bilayer deformations, it is difficult to unravel the complex mechanisms as the ion channel functions are sensitive to the properties of the surrounding lipid bilayers [6]. If deformation of the lipid bilayers is experimentally observed after applying MS, especially shear forces or compression, the stresses on the lipid bilayer and the ion channels can be estimated and related to the function of the involved molecules. By these MS, tilt of the average molecular orientation with respect to the layer was induced [7]. It is desired that the relationship between the angle of the lipid tilting and the ion channel activity could be surveyed when the lipid tilts. To obtain greater understanding of these mechanisms, measurement technologies to evaluate the deformations of lipid layers induced by physical and MS need to be developed.

Reconstructed systems of lipid bilayers are useful for investigating MS and the molecular functions because physiological molecular systems are too complex to clearly demonstrate the relationship. To study the distribution and dynamics of lipid bilayers, substrate-supported planar lipid bilayers (SPBs) have been fabricated [8, 9]. SPBs are advantageous because the cell membrane is produced on a flat substrate and can be easily observed using different measurement technologies such as atomic force microscopy (AFM), fluorescence imaging, and surface plasmon resonance (SPR) techniques because the configuration using flat substrate can be used in various biosensors. SPBs are useful systems for observing the deformation of lipid layers. Among the possible deformations occurring in lipid layers [6], we aim to detect tilted lipid bilayers on the substrate, which are related to membrane deformations such as curvature and thinning.

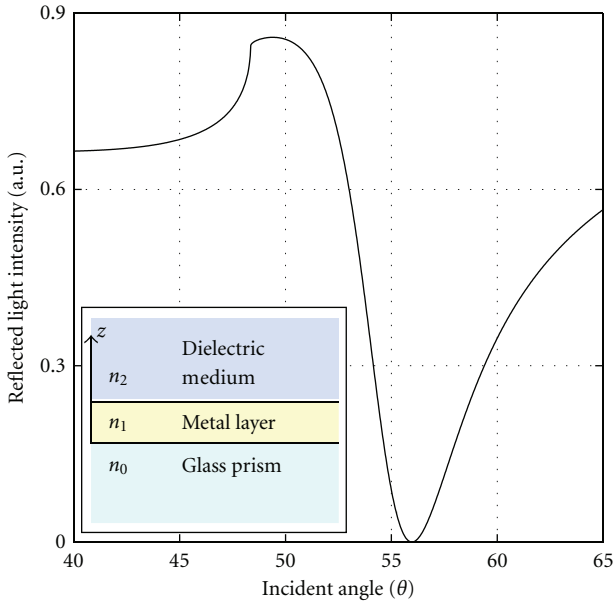

Figure 1: Reflected light intensity as a function of incident angle.

With regard to observing lipid bilayers, fluorescence imaging techniques [10, 11], AFM [12, 13], and SPR measurements [14–16] have been frequently used to understand lipid distributions and dynamics. Fluorescence imaging techniques have the disadvantage that fluorescent molecules are added to the system, which change the lipid molecules behavior due to perturbation with the fluorescent molecules. Moreover, it would be difficult to determine the tilt of the lipid bilayers from the fluorescence signal. Concerning AFM, the cantilever impedes the behavior of molecules on the lipid bilayers, and the contact imaging mode may damage the sample surface. Although noncontact imaging using AFM is possible, when the cantilever oscillates at a frequency slightly above its resonance frequency, the fluid flow on the substrate, which is necessary for exchanging the liquid sample, contributes to the oscillation noise. We believe that SPR is the best technique for lipid tilt observations because it enables noncontact and nonlabel measurements in liquid environments, has high thickness or refractive index resolution for detecting lipid bilayers, and allows the free flow of the fluid because there are no physical interactions with probes/cantilevers.

In lipid bilayer measurement using SPR, various parameters for the lipid bilayers, such as the thickness and interchain distance, affect the effective refractive index, which is detected using SPR. Therefore, to estimate the tilt angle of lipid bilayers from the experimental results and to obtain a better interpretation of the measured results, it is advantageous to know the relationship between the effective refractive index and the tilt angle for different thicknesses and interchain distances. In this paper, to derive such a relationship, we introduce a calculation model and simulate the changes in the effective refractive index due to the tilt angle of the lipid bilayers.

2. SPR Measurements

Surface plasmons are quanta of collective electron oscillations excited on a metal surface. They can be excited under the Kretschmann configuration [17], which consists of a high refractive index prism, coated with a thin metal layer and adjacent to a low-refractive-index dielectric medium (shown in inset of Figure 1). In this configuration, when light with p-polarization is provided from the side of the prism, surface plasmon can be efficiently coupled with light at the optimal incident angle. The reflected light intensity as a function of incident angle $R(\theta)$ can be calculated on the basis of the multiple-reflection theory [18, 19] as follows:

$$
\begin{aligned}
R(\theta) &= \left| \frac{r_{01}(\theta) + r_{12}(\theta)\exp[2ik_z(\theta)]}{1 + r_{01}(\theta)r_{12}(\theta)\exp[2ik_z(\theta)]} \right|^2, \\
k_z(\theta) &= \frac{2\pi}{\lambda} n_1 h \left[1 - \left(\frac{n_0}{n_1} \sin\theta \right)^2 \right]^{-1/2}, \\
r_{01}(\theta) &= \frac{n_0 \cos\theta - i\sqrt{n_0^2 \sin^2\theta - n_1^2}}{n_0 \cos\theta + i\sqrt{n_0^2 \sin^2\theta - n_1^2}}, \\
r_{12}(\theta) &= \frac{i\sqrt{n_0^2 \sin^2\theta - n_1^2} - n_2 \cos\theta'}{i\sqrt{n_0^2 \sin^2\theta - n_1^2} + n_2 \cos\theta'},
\end{aligned}
\tag{1}
$$

where k_z is the z component of the wave number for the light inside the metal; n_0, n_1, and n_2 denote the refractive index of the prism, metal, and low dielectric medium, respectively, λ is the wavelength of the incident light in vacuum, h denotes the thickness of the metal layer, and $r_{ij}(\theta)$, which is based on the Fresnel equations, is the amplitude reflectance at the boundary between the mediums i and j for light incident from i to j; and θ' denotes the refraction angle at the boundary between the metal layer and the dielectric medium.

Figure 1 shows the calculated results for the reflected light intensity. In the present calculation, we assume an excitation at 632.8 nm, a refractive index of 1.780 for the glass prism, a refractive index of 1.330 for the dielectric medium, and a 44 nm thick gold layer with a complex refractive index of $0.300 + 3.089\,i$ [20]. The influence of the gold layer thickness on the sensitivity of surface plasmon sensors is discussed in [21].

According to the plot, we can observe that the energy of the incident light is most efficiently absorbed at 56°, which is called the excitation angle of the surface plasmon θ_{sp}. This approach is advantageous because the excitation angle changes with the refractive index of the low-refractive-index medium n_2. It is well known that such excitation angle shifts are large enough to detect the adsorption of lipid bilayers. The changes in the detected refractive index δn_2 can be estimated from the relationship between θ_{sp} and n_2, as expressed in [22]

$$
\sin\theta_{sp} \approx \text{Real}\left(\frac{1}{n_g} \left(\frac{n_m^2 n_2^2}{n_m^2 + n_2^2} \right)^{1/2} \right), \tag{2}
$$

where n_g and n_m are the refractive index of glass and the complex refractive index of the metal, respectively.

The electric field induced by the surface plasmon penetrates the sample medium from the metal surface and can probe the changes in refractive index. The penetration depth, which is the measurement depth, is a few hundred nanometers. Since the measurement depth is larger than the thickness of the lipid bilayers, the detected value in the lipid measurement results in an effective refractive index n_{eff}, which can be defined as a weighted averaged refractive index over the measurement depth [23–25].

3. Calculation Model and Methods

3.1. Calculation Model. Figure 2 schematically depicts the model of the lipid bilayers on the substrate [26]. It consists of six layers: glass substrate, Au film, SiO_2, lower water layer, lipid bilayer, and upper water layer. The glass substrate and the Au film form the basic configuration for generating SPRs. The SiO_2 layer is used for preserving the hydrophilic nature of the surface of the substrate and to form bilayer without defects on the hydrophilic surface [20]. Because the combined thickness of the SiO_2 layer, water layers, and lipid bilayer is less than the measurement depth, the obtained n_{eff} is averaged across the SiO_2 layer, both water layers, and the lipid bilayer.

In the model, α is the tilt of the lipid bilayers. To determine the refractive index of the lipid bilayer, the following equation is used:

$$n^2 = \varepsilon, \tag{3}$$

where ε denotes the permittivity of the lipid bilayers. The lipid bilayer has anisotropic permittivity, with components $\varepsilon_\perp$ and $\varepsilon_\parallel$ representing the permittivity perpendicular and parallel to the substrate, respectively, at $\alpha = 0^\circ$. In the SPR measurements, permittivity parallel to the substrate can be ignored [27]. Therefore, (3) can be expressed using $\varepsilon_\perp$ as follows:

$$n_{\text{spr}} = \sqrt{\varepsilon_\perp}, \tag{4}$$

where n_{spr} denotes the refractive index of the lipid bilayers detected in the SPR measurements. At $\alpha = 90^\circ$, because $\varepsilon_\perp$ is equal to $\varepsilon_\parallel$, (4) is rewritten as follows:

$$n'_{\text{spr}} = \sqrt{\varepsilon_{||}}. \tag{5}$$

To express n_{spr} in terms of the tilt angle α on the basis of the results of SPR measurement for tilted anisotropic molecules (liquid crystal cells) [28, 29], we assume that the value of $\varepsilon_\perp$ linearly changes to $\varepsilon_{||}$ in the range from $\alpha = 0^\circ$ to $\alpha = 90^\circ$, provided that $\varepsilon_\perp > \varepsilon_{||}$, given as

$$n^2_{\text{spr}} = \varepsilon_{\text{spr}} = \frac{\varepsilon_{||} - \varepsilon_\perp}{90} \times \alpha + \varepsilon_\perp. \tag{6}$$

3.2. Calculation Method. The calculation process used to determine the effective refractive index as a function of the tilt of lipid bilayers is presented here. The calculation procedure is as follows: (1) the reflected light intensities are calculated as a function of incident angle for the model shown in Figure 2 with $\alpha = 0^\circ$; (2) θ_{sp} is estimated and n_{eff} is derived using (2); (3) α is increased in 1° steps, and the refractive index and the thickness t of the lipid bilayers are calculated using (6) and $t = t_0 \cos\alpha$, respectively, which are set as the model parameters; (4) steps (1)–(3) are performed for tilt angles 0°–50°. The effective refractive index detected is normalized by the refractive index of water (1.330) over the metal surface. The calculation range of the tilt angle is determined on the basis of the idea that lipid bilayers with small tilt angles are typically discussed in studies on lipid functionalities [30]. Moreover, lipid bilayers with large tilt angles are structurally inconsistent with real cell membrane, and it would be difficult to keep such lipids in a bilayer form.

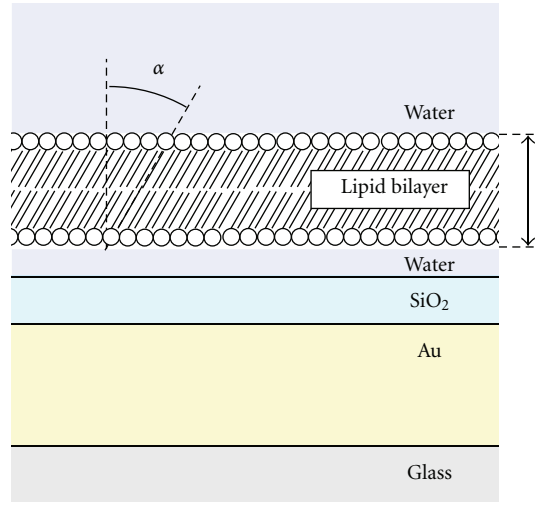

Figure 2: Model to calculate effective refractive index as a function of tilt angle α.

4. Results and Discussion

4.1. Thickness and Refractive Index of Lipid Bilayers as a Function of Tilt Angle. Figures 3(a) and 3(b) show the thickness and refractive index plots as a function of tilt angle, respectively. In this calculation, we used the same parameters for the refractive index that were used in Section 2. The refractive index of SiO_2 is assumed to be 1.515, and the thicknesses of the Au film and the SiO_2 layer are assumed to be 44 and 12 nm, respectively [20]. The thickness of the lipid bilayer, t_0, is set as 5 nm because the structure of a fully hydrated lipid bilayer has been estimated at around 5 nm [31] and also because it has been experimentally confirmed by AFM [32]. The anisotropic permittivity of the lipid bilayers varies with the interchain distance d. We set d as 0.500 nm, as this value has been usually assumed for liquid paraffins [33]. The values of $\varepsilon_\perp$ and $\varepsilon_\parallel$ are 2.288 and 2.124, respectively [33].

According to the plots in Figures 3(a) and 3(b), the thickness and refractive index of the lipid bilayers decrease with increasing tilt angles. Hence, it is expected that the effective refractive index decreases with increasing tilt angles.

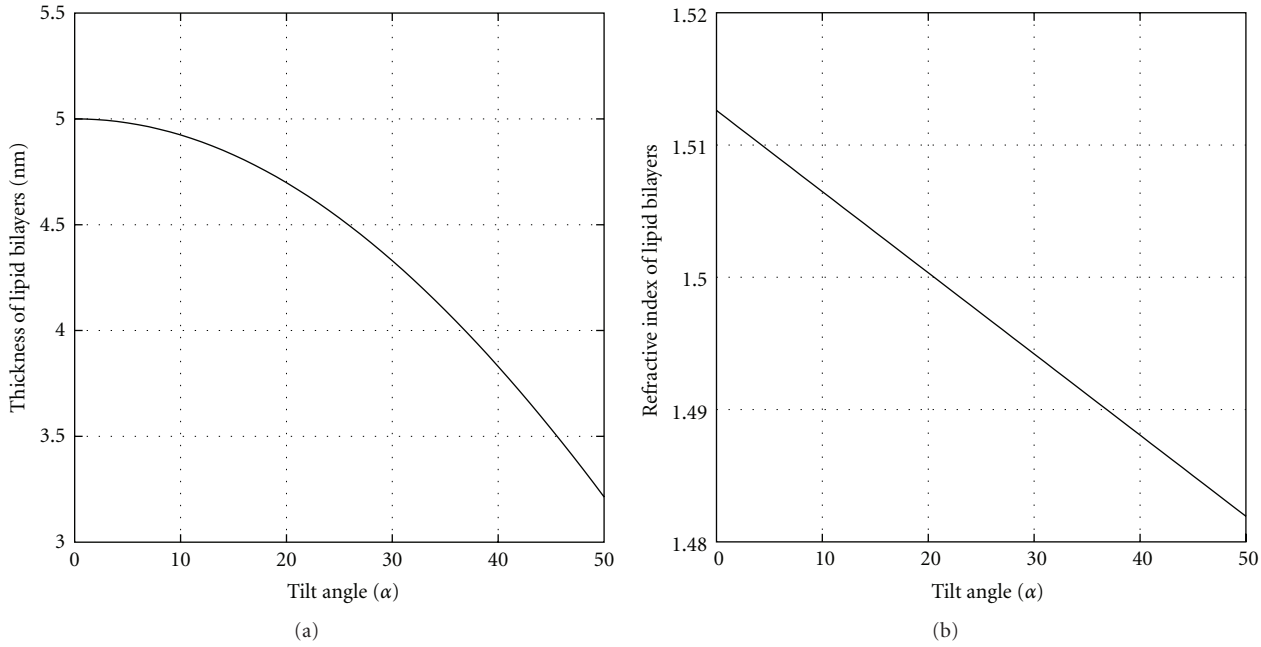

Figure 3: (a) Thickness of lipid bilayers as a function of tilt angle. (b) Refractive index as a function of tilt angle.

4.2. Effective Refractive Index as a Function of Tilt Angle. Based on the model in Figure 2 and the calculation method described in Section 3, we calculated the effective refractive index as a function of tilt angle. In the calculation, the thickness of lipid bilayers t and that of refractive index parameters for each tilt angle α are taken from the plots in Figures 3(a) and 3(b). The calculated results when $d = 0.500$ nm and $t_0 = 5$ nm, shown in the red plot in Figure 4, indicate that the effective refractive index decreases with increasing tilt angles. When the tilt angle is between 0° and 10°, the change in the effective refractive index is 4.8×10^{-4}. This value is large enough to distinguish differences of five degrees if we assume SPR with the refractive index resolution of 1.0×10^{-4} [34].

To further investigate the resolution and sensitivity effects, the interchain distance d was varied slightly to 0.475 nm, a value referred to in [33]. We also varied the thickness t_0 to 3 nm, which is the value measured by localized SPR microscopy [20]. The green line shows the results using $t_0 = 5$ nm at $d = 0.475$ nm, which has an anisotropic permittivity of $\varepsilon_\perp = 2.534$ and $\varepsilon_\parallel = 2.245$ [33]. The pink and blue plots show the results for $t_0 = 3$ nm at $d = 0.475$ nm and $t_0 = 3$ nm at $d = 0.500$ nm, respectively. These results show that the n_{eff} slopes are steeper with increasing thickness and anisotropic permittivity, that is, increasing thickness and anisotropic permittivity provides more sensitive measurements for the tilt of the lipid bilayers.

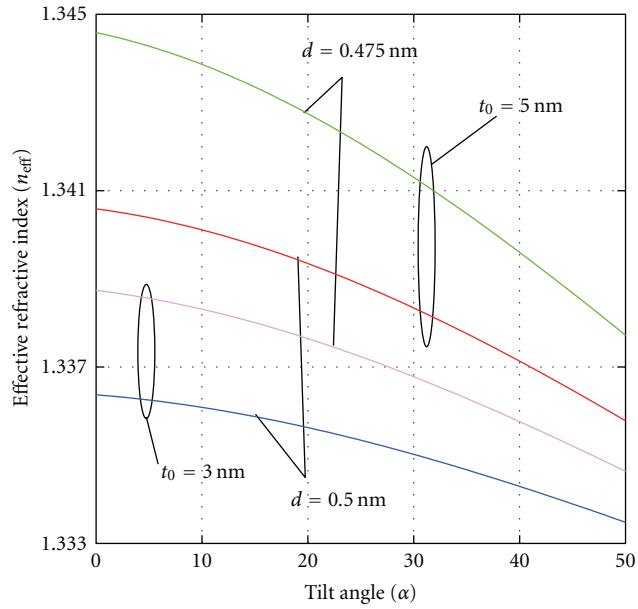

Figure 4: Calculated plots of effective refractive index as function of tilt angle for thickness $t_0 = 3.0$ and 5.0 nm and interchain distance $d = 0.475$ and 0.500 nm.

5. Conclusion

We theoretically identified the relationship between the effective refractive index and tilt angle of lipid bilayers and demonstrated how the tilt angle of the lipid bilayers on the substrate can be detected using SPR techniques. We also showed that the detection sensitivity changes due to lipid bilayers with different thickness and anisotropic permittivity. This insight can contribute for detection of lipid tilting by shear force or compression to SPBs that contains transmembrane mechanosensing ion channel. Using this measurement technology, the relationship between the angle of the lipid tilting and the ion channel activity could be surveyed when the lipid tilts.

Acknowledgments

This study was partly supported by a grant-in-aid for Scientific Research for Young Scientists (A) (no. 22680036 to K. Matsuura) and by the Special Coordination Funds for Promoting Sciences and Technology from the Ministry of Education, Science, Sports, and Culture, Japan.

References

[1] R. Inoue, Z. Jian, and Y. Kawarabayashi, "Mechanosensitive TRP channels in cardiovascular pathophysiology," *Pharmacology and Therapeutics*, vol. 123, no. 3, pp. 371–385, 2009.

[2] S. I. Sukharev, B. Martinac, V. Y. Arshavsky, and C. Kung, "Two types of mechanosensitive channels in the *Escherichia coli* cell envelope: solubilization and functional reconstitution," *Biophysical Journal*, vol. 65, no. 1, pp. 177–183, 1993.

[3] B. Corry and B. Martinac, "Bacterial mechanosensitive channels: experiment and theory," *Biochimica et Biophysica Acta*, vol. 1778, no. 9, pp. 1859–1870, 2008.

[4] C. A. Guyton and E. J. Hall, *Textbook of Medical Physiology*, WB Saunders, 11th edition, 2005.

[5] K. Matsuura, N. Hayashi, Y. Kuroda et al., "Improved development of mouse and human embryos using a tilting embryo culture system," *Reproductive BioMedicine Online*, vol. 20, no. 3, pp. 358–364, 2010.

[6] D. Reeves, T. Ursell, P. Sens, J. Kondev, and R. Phillips, "Membrane mechanics as a probe of ion-channel gating mechanisms," *Physical Review E*, vol. 78, no. 4, Article ID 041901, 11 pages, 2008.

[7] A. Jákli, J. Harden, C. Notz, and C. Bailey, "A possible mechanism for mechano-, and magneto-receptions in biology," *Electronic-Liquid Crystal Communications*. In press.

[8] D. Cao and H. Meier, "Patterning solid-supported lipid bilayer membranes by lithographic polymerization of a diacetylene lipid," *Angewandte Chemie—International Edition*, vol. 40, no. 1, pp. 172–174, 2001.

[9] E. Sackmann, "Supported membranes: scientific and practical applications," *Science*, vol. 271, no. 5245, pp. 43–48, 1996.

[10] M. Loesche, E. Sackmann, and H. Moehwald, "A fluorescence microscopic study concerning the phase diagram of phospholipids," *Berichte der Bunsengesellschaft*, vol. 87, no. 10, pp. 848–852, 1983.

[11] R. M. Weis and H. M. McConnell, "Two-dimensional chiral crystals of phospholipid," *Nature*, vol. 310, no. 5972, pp. 47–49, 1984.

[12] W. C. Lin, C. D. Blanchette, T. V. Ratto, and M. L. Longo, "Lipid asymmetry in DLPC/DSPC-supported lipid bilayers: a combined AFM and fluorescence microscopy study," *Biophysical Journal*, vol. 90, no. 1, pp. 228–237, 2006.

[13] R. P. Richter and A. R. Brisson, "Following the formation of supported lipid bilayers on Mica: a study combining AFM, QCM-D, and ellipsometry," *Biophysical Journal*, vol. 88, no. 5, pp. 3422–3433, 2005.

[14] B. Rothenhäusler and W. Knoll, "Surface-plasmon microscopy," *Nature*, vol. 332, no. 6165, pp. 615–617, 1988.

[15] B. Rothenhäusler, C. Duschl, and W. Knoll, "Plasmon surface polariton fields for the characterization of thin films," *Thin Solid Films*, vol. 159, no. 1-2, pp. 323–330, 1988.

[16] W. Hickel and W. Knoll, "Surface plasmon microscopy of lipid layers," *Thin Solid Films*, vol. 187, no. 2, pp. 349–356, 1990.

[17] E. Kretschmann and H. Raether, "Radiative decay of nonradiative surface plasmons excited by light," *Zeitschrift für Naturforschung*, vol. 23, pp. 2135–2136, 1968.

[18] N. J. Harrick, *Internal Reflection Spectroscopy*, John Wiley & Sons, New York, NY, USA, 1967.

[19] H. Kano and S. Kawata, "Surface-plasmon sensor for absorption-sensitivity enhancement," *Applied Optics*, vol. 33, no. 22, pp. 5166–5170, 1994.

[20] K. Watanabe, M. Ryosuke, G. Terakado, T. Okazaki, K. Morigaki, and H. Kano, "High resolution imaging of patterned model biological membranes by localized surface plasmon microscopy," *Applied Optics*, vol. 49, no. 5, pp. 887–891, 2010.

[21] S. Ekgasit, C. Thammacharoen, F. Yu, and W. Knoll, "Influence of the metal film thickness on the sensitivity of surface plasmon resonance biosensors," *Applied Spectroscopy*, vol. 59, no. 5, pp. 661–667, 2005.

[22] H. Raether, *Surface Plasmons on Smooth and Rough Surfaces and on Gratings*, Springer, Berlin, Germany, 1988.

[23] L. S. Jung, C. T. Campbell, T. M. Chinowsky, M. N. Mar, and S. S. Yee, "Quantitative interpretation of the response of surface plasmon resonance sensors to adsorbed films," *Langmuir*, vol. 14, no. 19, pp. 5636–5648, 1998.

[24] J. S. Shumaker-Parry and C. T. Campbell, "Quantitative methods for spatially resolved adsorption/desorption measurements in real time by surface plasmon resonance microscopy," *Analytical Chemistry*, vol. 76, no. 4, pp. 907–917, 2004.

[25] K. Watanabe, "Sensitivity optimization of surface plasmon sensors for detection of intermediate layers," *Sensors and Actuators, A*, vol. 173, no. 1, pp. 36–40, 2012.

[26] K. Watanabe, "Model for measurement of water layer thickness under lipid bilayers by surface plasmon resonance," *Biomedical Optics Express*, vol. 2, pp. 1115–1120, 2011.

[27] W. Lukosz, "Integrated-optical and surface-plasmon sensors for direct affinity sensing. Part II: anisotropy of adsorbed or bound protein adlayers," *Biosensors and Bioelectronics*, vol. 12, no. 3, pp. 175–184, 1997.

[28] A. Baba, F. Kaneko, K. Shinbo, K. Kato, S. Kobayashi, and T. Wakamatsu, "Evaluation of tilt angles of nematic liquid crystal molecules on polyimide Langmuir-Blodgett films using the attenuated total reflection measurement method," *Japanese Journal of Applied Physics, Part 1*, vol. 37, no. 5, pp. 2581–2586, 1998.

[29] A. Baba, F. Kaneko, K. Shinbo, T. Wakamatsu, K. Kato, and S. Kobayashi, "Evaluation of temperature and voltage dependences of nematic liquid crystal molecules on Langmuir-Blodgett films in the thick cell using the attenuated total reflection method," *Materials Science and Engineering C*, vol. 8-9, pp. 145–150, 1999.

[30] S. May, "Protein-induced bilayer deformations: the lipid tilt degree of freedom," *European Biophysics Journal*, vol. 29, no. 1, pp. 17–28, 2000.

[31] J. F. Nagle and S. Tristram-Nagle, "Structure of lipid bilayers," *Biochimica et Biophysica Acta*, vol. 1469, no. 3, pp. 159–195, 2000.

[32] K. Morigaki, H. Schönherr, and T. Okazaki, "Polymerization of diacetylene phospholipid bilayers on solid substrate: influence of the film deposition temperature," *Langmuir*, vol. 23, no. 24, pp. 12254–12260, 2007.

[33] W. Huang and D. G. Levitt, "Theoretical calculation of the dielectric constant of a bilayer membrane," *Biophysical Journal*, vol. 17, no. 2, pp. 111–128, 1977.

[34] J. Homola, *Surface Plasmon Resonance Based Sensors*, Springer, Berlin, Germany, 2006.